AMERICAN SOCIETY FOR MICROBIOLOGY | mBio®

RESEARCH ARTICLE
Ecological and Evolutionary Science

Long-Term Transcriptional Activity at Zero Growth of a Cosmopolitan Rare Biosphere Member

Bela Hausmann,[a,b] Claus Pelikan,[a] Thomas Rattei,[c] Alexander Loy,[a] Michael Pester[b,d,e]

[a]Research Network Chemistry meets Microbiology, Department of Microbiology and Ecosystem Science, Division of Microbial Ecology, University of Vienna, Vienna, Austria

[b]Department of Biology, University of Konstanz, Konstanz, Germany

[c]Research Network Chemistry meets Microbiology, Department of Microbiology and Ecosystem Science, Division of Computational Systems Biology, University of Vienna, Vienna, Austria

[d]Department of Microorganisms, Leibniz Institute DSMZ, Braunschweig, Germany

[e]Institute of Microbiology, Technical University of Braunschweig, Braunschweig, Germany

ABSTRACT Microbial diversity in the environment is mainly concealed within the rare biosphere (all species with <0.1% relative abundance). While dormancy explains a low-abundance state very well, the mechanisms leading to rare but active microorganisms remain elusive. We used environmental systems biology to genomically and transcriptionally characterize "*Candidatus* Desulfosporosinus infrequens," a low-abundance sulfate-reducing microorganism cosmopolitan to freshwater wetlands, where it contributes to cryptic sulfur cycling. We obtained its near-complete genome by metagenomics of acidic peat soil. In addition, we analyzed anoxic peat soil incubated under *in situ*-like conditions for 50 days by *Desulfosporosinus*-targeted qPCR and metatranscriptomics. The *Desulfosporosinus* population stayed at a constant low abundance under all incubation conditions, averaging 1.2×10^6 16S rRNA gene copies per cm^3 soil. In contrast, transcriptional activity of "*Ca.* Desulfosporosinus infrequens" increased at day 36 by 56- to 188-fold when minor amendments of acetate, propionate, lactate, or butyrate were provided with sulfate, compared to the no-substrate-control. Overall transcriptional activity was driven by expression of genes encoding ribosomal proteins, energy metabolism, and stress response but not by expression of genes encoding cell growth-associated processes. Since our results did not support growth of these highly active microorganisms in terms of biomass increase or cell division, they had to invest their sole energy for maintenance, most likely counterbalancing acidic pH conditions. This finding explains how a rare biosphere member can contribute to a biogeochemically relevant process while remaining in a zero-growth state over a period of 50 days.

IMPORTANCE The microbial rare biosphere represents the largest pool of biodiversity on Earth and constitutes, in sum of all its members, a considerable part of a habitat's biomass. Dormancy or starvation is typically used to explain the persistence of low-abundance microorganisms in the environment. We show that a low-abundance microorganism can be highly transcriptionally active while remaining in a zero-growth state for at least 7 weeks. Our results provide evidence that this zero growth at a high cellular activity state is driven by maintenance requirements. We show that this is true for a microbial keystone species, in particular a cosmopolitan but permanently low-abundance sulfate-reducing microorganism in wetlands that is involved in counterbalancing greenhouse gas emissions. In summary, our results provide an important step forward in understanding time-resolved activities of rare biosphere members relevant for ecosystem functions.

KEYWORDS cryptic sulfur cycle, growth arrest, keystone species, maintenance, metatranscriptome, peatland

Citation Hausmann B, Pelikan C, Rattei T, Loy A, Pester M. 2019. Long-term transcriptional activity at zero growth of a cosmopolitan rare biosphere member. mBio 10:e02189-18. https://doi.org/10.1128/mBio.02189-18.

Editor Mark J. Bailey, CEH-Oxford

Address correspondence to Alexander Loy, loy@microbial-ecology.net, or Michael Pester, michael.pester@dsmz.de.

Received 8 October 2018
Accepted 4 January 2019
Published 12 February 2019

The vast majority of microbial diversity worldwide is represented by the rare biosphere (1–4). This entity of microorganisms consists of all microbial species that have an arbitrarily defined relative population size of <0.1% in a given habitat at a given time (1–4). The rare biosphere is opposed by a much smaller number of moderately abundant or very abundant microbial species (≥0.1% and ≥1.0% relative abundance, respectively) (5), which are thought to be responsible for the major carbon and energy flow through a habitat as based on their cumulative biomass. However, there is accumulating experimental evidence that the rare biosphere is not just a "seed bank" of microorganisms that are waiting to become active and numerically dominant upon environmental change (3, 6) but also harbors metabolically active microorganisms with important ecosystem functions (4).

First hints for metabolically active rare biosphere members were evident from seasonal patterns of marine bacterioplankton species. Here, many taxa that displayed recurring annual abundance changes were of low abundance and even during their bloom periods never reached numerically abundant population sizes (7–9). In soil environments, removal of low-abundance species by dilution-to-extinction had a positive effect on intruding species, suggesting that active low-abundance species preoccupy ecological niches and thus slow down invasion (10–12). Soil microorganisms of low relative abundance were also shown to play a role in community-wide species interactions, e.g., by being involved in the production of antifungal compounds that protect plants from pathogens (13) or by constituting the core of microorganisms that respond to the presence of a particular plant species (14). Other examples include microorganisms with a specialized metabolism that sustain stable low-abundance populations in an ecosystem (3). For example, N_2-fixing microorganisms in the ocean (15) or sulfate-reducing microorganisms (SRM) in peatlands (5, 16, 17) were shown to fulfill such key functions.

A peatland *Desulfosporosinus* species was one of the first examples identified as an active rare biosphere member contributing to an important ecosystem function (16). This SRM is involved in the cryptic sulfur cycle of peatlands (5, 16), which in turn controls the emission of the greenhouse gas CH_4 from these globally relevant environments (17). Although porewater sulfate concentrations are typically quite low in peatlands (<300 μM) (17), these environments are characterized by temporally fluctuating high sulfate reduction rates (up to 1,800 nmol cm^{-3} day^{-1}) (17). These rates can be in the same range as in sulfate-rich marine surface sediments, where sulfate reduction is one of the major anaerobic carbon degradation pathways (18, 19). In low-sulfate peatlands, such high sulfate reduction rates can be maintained only by rapid aerobic or anaerobic reoxidation of reduced sulfur species back to sulfate (17). Since SRM generally outcompete methanogens and syntrophically associated fermenters (20), they exert an important intrinsic control function on peatland CH_4 production (21–23). This is important, since natural wetlands, such as peatlands, are estimated to be responsible for 30% of the annual emission of this potent greenhouse gas (24–26).

Little is known about the ecophysiology of metabolically active but low-abundance microorganisms. This lack of knowledge is clearly founded in their low numerical abundance, making it inherently difficult to study their metabolic responses or even to retrieve their genomes directly from the environment. In a preceding study, we could show that the low-abundance peatland *Desulfosporosinus* species mentioned above follows an ecological strategy to increase its cellular ribosome content while maintaining a stable low-abundance population size when exposed to favorable, sulfate-reducing conditions (5). This was unexpected since metabolic activity in bacteria and archaea is typically followed by growth (in terms of cell division or biomass increase) if they are not severely energy or nutrient limited (27) or engaged in major maintenance processes coping with (environmental) stress (28). The studied *Desulfosporosinus* species is found worldwide in a wide range of low-sulfate wetlands, including peatlands, permafrost soils, and rice paddy fields (5). This emphasizes its importance as a model organism for active rare biosphere members. In this study, we used an environmental systems biology approach to deepen our understanding of the cellular biology of this

rare biosphere member. In particular, we retrieved its genome by metagenomics from native and incubated peat soil and followed its transcriptional responses in peat soil microcosms simulating transient *in situ* conditions, i.e., sulfate-reducing or methanogenic conditions in the background of minor amendments of the organic carbon degradation intermediate formate, acetate, propionate, lactate, or butyrate.

RESULTS

A near-complete genome of a rare biosphere member from peat soil. We obtained the population genome of the low-abundance *Desulfosporosinus* species by coassembly and differential coverage binning of metagenomes obtained from native peat soil and ^{13}C-labeled fractions of a DNA-stable isotope probing experiment of the same peatland (see Fig. S1 in the supplemental material) (29). The high-quality metagenome-assembled genome (MAG) SbF1 had a size of 5.3 Mbp (on 971 scaffolds), a G+C content of 42.6%, a CheckM-estimated completeness of 98.0%, a potential residual contamination of 3.9%, and 10% strain heterogeneity. Besides 16S and 23S rRNA genes, SbF1 carried 6,440 protein-coding genes (CDS), five 5S rRNA gene copies, 59 tRNAs, and 37 other ncRNAs, making a total of 6,543 predicted genomic features. The genome size and G+C content were in the same range as observed for genomes of cultured *Desulfosporosinus* species (3.0 to 5.9 Mbp and 42 to 44%, respectively) (30–34). Scaffolds containing rRNA genes had a higher coverage than the average coverage of all scaffolds (Fig. S1), indicating multiple *rrn* operon copies, as is known from genomes of other *Desulfosporosinus* species (on average, 9.3 *rrn* operons; range, 8 to 11) (35).

16S rRNA-based phylogenetic tree reconstruction placed SbF1 into a well-supported clade together with *Desulfosporosinus* sp. strain 44a-T3a (98.3% sequence identity), *Desulfosporosinus* sp. strain OT (98.8%), and *Desulfosporosinus* sp. strain 5apy (98.1%). The most similar validly described species was *Desulfosporosinus lacus* with a sequence identity of 97.5% (Fig. S2a). Phylogenomics confirmed *Desulfosporosinus* sp. OT as the closest relative (Fig. S2b) with average amino and nucleic acid identities (AAI and ANI, respectively) of 77% and 79%, respectively (Fig. S3). The intragenus AAI variability of *Desulfosporosinus* species was 69 to 93% (Fig. S3). Therefore, MAG SbF1 represents a novel species in this genus based on species-level thresholds of 99% for the 16S rRNA gene (36) and 96.5% for ANI (37).

The versatile energy metabolism of the low-abundance *Desulfosporosinus*. *Desulfosporosinus* sp. MAG SbF1 encoded the complete canonical pathway for dissimilatory sulfate reduction (Fig. 1 and Table S1a). This encompassed sulfate adenylyltransferase (Sat), adenylyl-sulfate reductase (AprBA), dissimilatory sulfite reductase (DsrAB), and sulfide-releasing DsrC, which are sequentially involved in the reduction of sulfate to sulfide. In addition, genes encoding the electron-transferring QmoAB and DsrMKJOP complexes were detected, with their subunit composition being typical for *Desulfosporosinus* species (30, 31, 33, 34). Other *dsr* genes included *dsrD*, *dsrN*, and *dsrT* (38), with hitherto-unvalidated function; *fdxD*, which encodes a [4Fe4S]-ferredoxin; and a second set of DsrMK family-encoding genes (*dsrM2* and *dsrK2*). SbF1 also encoded the trimeric dissimilatory sulfite reductase AsrABC (anaerobic sulfite reductase) (39).

SbF1 carried genes to utilize lactate, propionate, acetate, formate, or H_2 as electron donors (Fig. 1). All enzymes necessary for propionate oxidation to the central metabolite pyruvate (including those belonging to a partial citric acid cycle) were encoded on two scaffolds (Table S1a). For lactate utilization, SbF1 carried three paralogs of glycolate/D-lactate/L-lactate dehydrogenase family genes (*lutDF*/*glcDF*). However, the substrate specificity of the encoded enzymes could not be inferred from sequence information alone. The transcription of *lutDF* and *lutD_2* was stimulated by the addition of L-lactate (Fig. 1), which indicates that these genes encode functional lactate dehydrogenases (LDHs). The third paralog (*glcDF*, Table S1a) was not stimulated by lactate. LutDF was organized in an operon with a lactate permease (LutP) and a lactate regulatory gene (*lutR*). LutD_2 was organized in an operon with an electron-transferring flavoprotein (EtfBA_2), which resembled the electron-confurcating LDH/Etf complex in

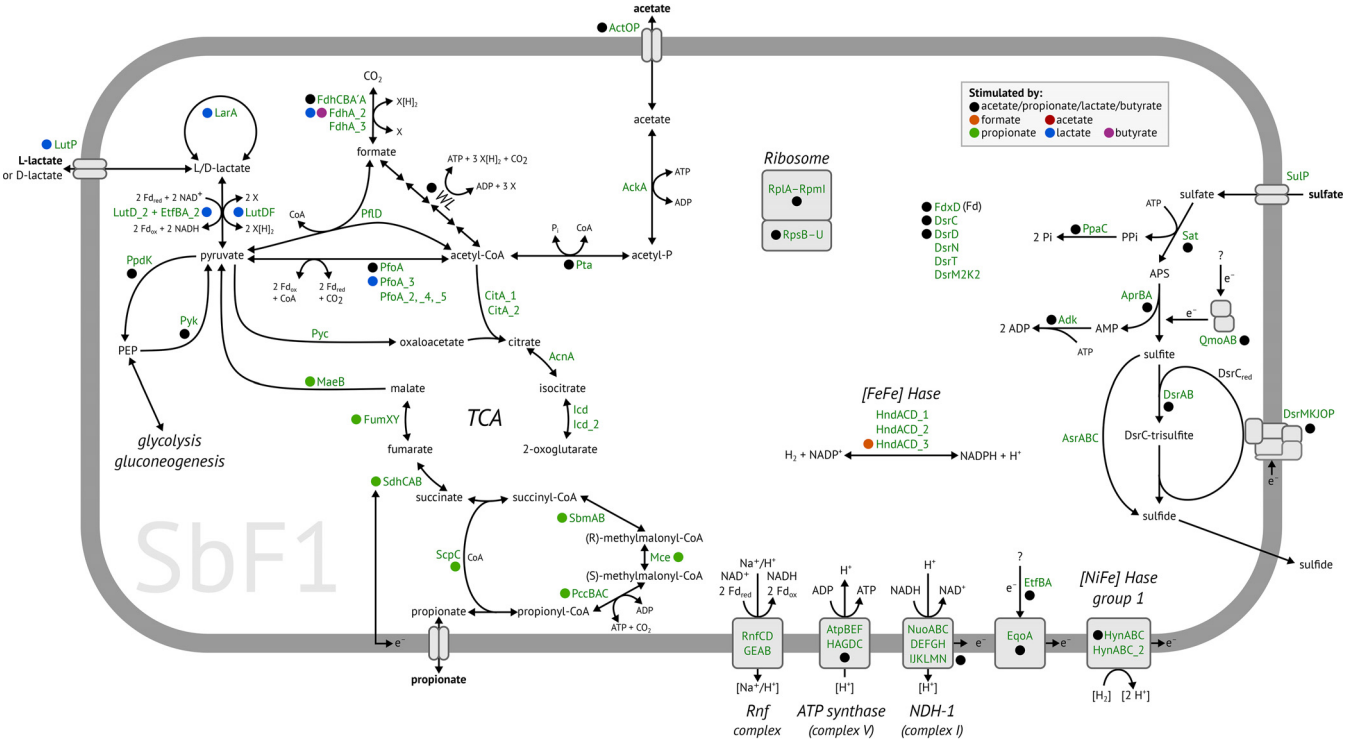

FIG 1 Metabolic model of *Desulfosporosinus* sp. MAG SbF1. Gene expression stimulated by specific substrates in combination with sulfate is indicated by colored points. Paralogous genes are indicated by an underscore followed by a number. Plus signs indicates proposed protein complexes. Details for all genes are given in Table S1a, and transcription patterns are shown in Fig. 4. For the citric acid cycle and anaplerotic reactions, carriers of reducing equivalents and further by-products are not shown. The following abbreviations were used: X, unknown reducing equivalent carrier, e.g., NAD^+ or ferredoxin; WL, Wood-Ljungdahl pathway consisting of enzymes encoded by the *acs* operon, MetF, FolD, FchA, and Fhs; TCA, citric acid cycle; FDH, formate dehydrogenase; Hase, hydrogenase; NDH-1, NADH dehydrogenase 1; LDH, lactate dehydrogenase.

Acetobacterium woodii (40). LDHs have been shown to utilize both L- and D-lactate (40, 41). However, SbF1 also encoded a lactate racemase (LarA) and a lactate racemase-activating system (LarEBC) for interconversion of both stereoisomers (42).

Pyruvate, the intermediate product in propionate and lactate degradation, can be further oxidized to acetyl-CoA with either one of several pyruvate-ferredoxin oxidoreductases (PfoA) or formate C-acetyltransferase (PflD). Acetyl-CoA can then be completely oxidized to CO_2 via the Wood-Ljungdahl pathway (43), which is complete in SbF1 (Fig. 1; Table S1a) and present in the genomes of all other sequenced *Desulfosporosinus* species (30, 31, 33, 34). Alternatively, acetyl-CoA may be incompletely oxidized to acetate via acetyl-phosphate by phosphate acetyltransferase (Pta) and acetate kinase (AckA). Pta and AckA are bidirectional enzymes, opening the possibility that acetate could be degraded via these two enzymes and the downstream Wood-Ljungdahl pathway to CO_2.

Formate and H_2 represented additional potential electron donors for SbF1. Its genome encoded three formate dehydrogenases (FDH). FDH-1 consists of three subunits (*fdhCBA*), while FDH-2 (FdhA_2) and FDH-3 (FdhA_3) are monomeric enzymes. In addition, [NiFe] hydrogenases of group 1 and 4f, as well as [FeFe] hydrogenases of group A (44), were encoded. Homologs of genes for butyrate oxidation were missing in SbF1 (45), which is in contrast to other *Desulfosporosinus* species (e.g., *Desulfosporosinus orientis*). Both glycolysis and gluconeogenesis were complete. However, neither a glucokinase nor a phosphotransferase system (PTS) was found. Coupling of electron transfer to energy conservation could be mediated in SbF1 by a H^+/Na^+-pumping Rnf complex (RnfCDGEAB) (46) and an NADH dehydrogenase (respiratory complex I, NuoABCDEFGHIJKLMN). In addition, the complete gene set for ATP synthase (AtpABCDEFGH) was identified (Fig. 1; Table S1a).

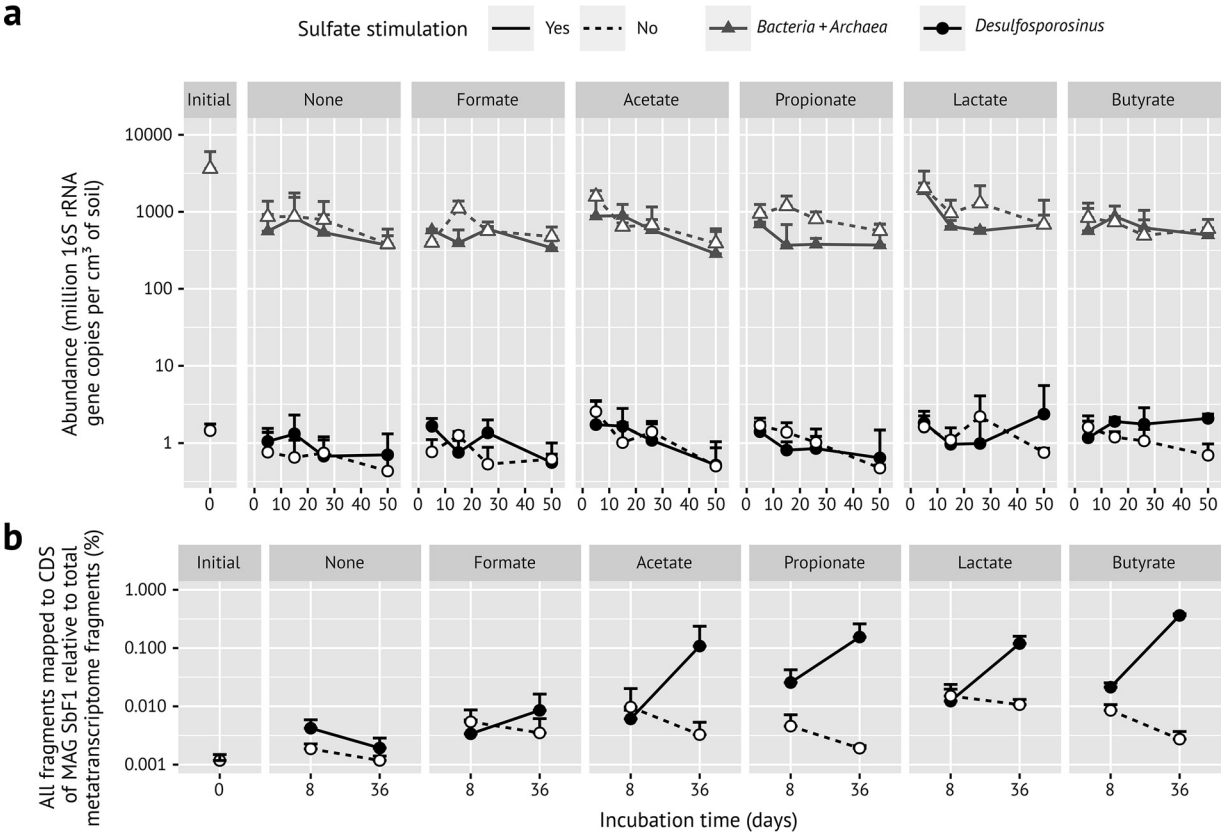

FIG 2 (a) Time-resolved absolute abundance of the *Desulfosporosinus* population (black circles) compared to all *Bacteria* and *Archaea* (gray triangles) in anoxic peat soil microcosms under various *in situ*-like conditions as determined by quantitative PCR (modified from reference 5). Error bars represent 1 standard deviation of the mean ($n = 3$; $n = 2$ for propionate with sulfate stimulation, all days, and butyrate with sulfate stimulation, day 50). (b) Corresponding overall transcriptional changes (mRNA of all CDS) of *Desulfosporosinus* sp. MAG SbF1 in the same anoxic microcosms. Error bars represent 1 standard deviation of the mean ($n = 3$; $n = 2$ for propionate with sulfate stimulation).

Long-term transcriptional activity of *Desulfosporosinus* sp. MAG SbF1 at zero growth. Naturally occurring hot spots of sulfate-reducing activity in peat soil (47–50) were mimicked by periodically amending sulfate in the lower- micromolar range to anoxic peat microcosms (every 3 to 7 days) and comparing this to unamended (i.e., methanogenic) control microcosms. In addition, sulfate-reducing and methanogenic microcosms received, in triplicates, periodic amendments of either formate, acetate, propionate, lactate, or butyrate compared to controls without amendment. Substrate supply did generally not exceed 100 to 200 μM, thus again mimicking *in situ* concentrations of these naturally occurring organic carbon degradation intermediates in peatlands (5). The overall *Desulfosporosinus* population remained stable throughout the incubation period in the various microcosms (on average, 1.2×10^6 16S rRNA gene copies per cm^3 of soil [Fig. 2a]). Compared to the total bacterial and archaeal community, this resembled a relative abundance of 0.018% when corrected for the average 9.3 *rrn* operons per genome in the genus *Desulfosporosinus* (35). The 16S rRNA gene of *Desulfosporosinus* sp. MAG SbF1 was 100% identical to OTU0051, which dominated the *Desulfosporosinus* population as evident from a previously published 16S rRNA (gene) amplicon survey of the same microcosms (74% of all *Desulfosporosinus* amplicons) (5). In contrast to its stable low abundance, the overall *Desulfosporosinus* population substantially increased its 16S rRNA copy numbers by 2.2, 4.9, 5.9, or 13.6-fold in sulfate-reducing incubations stimulated by either acetate, propionate, lactate, or butyrate, respectively. In contrast, *Desulfosporosinus* 16S rRNA copy numbers remained stable or even slightly decreased in the sulfate-amended no-substrate control and the methanogenic incubations (Fig. S4) (5). Again, these increases were mainly reflected in

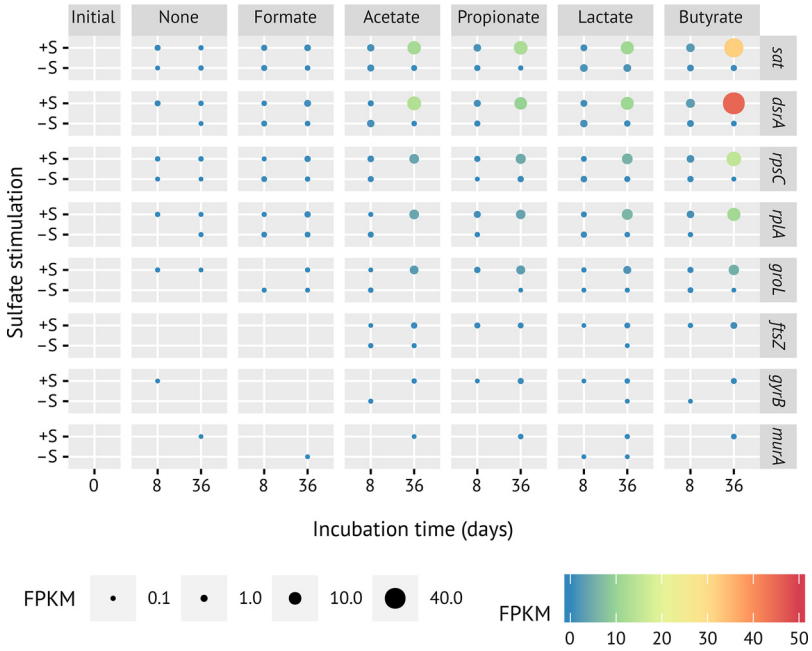

FIG 3 Time-resolved transcriptional changes of selected genes representing the sulfate reduction pathway (*sat*, *dsrA*), ribosomal proteins of the large (*rplA*) and small (*rpsC*) subunit, the GroEL chaperon (*groL*), cell division (*ftsZ*), DNA replication (*gyrB*), and peptidoglycan synthesis (*murA*). Panels represent the various substrate incubations: initial, initial peat soil to set up peat microcosms; +/−S, incubations with or without external sulfate, respectively. The size and color of the dots represent average FPKM values of the respective normalized gene expression.

changes of OTU0051 (*Desulfosporosinus* sp. MAG SbF1) as shown in the amplicon study mentioned above (5).

We used metatranscriptomics of the same microcosms to analyze whether this strong increase in 16S rRNA copies at zero growth was accompanied by gene expression of metabolic pathways and cell growth-associated processes in *Desulfosporosinus* sp. MAG SbF1. Compared to the initial soil, the overall transcriptional activity of SbF1 steadily increased at days 8 and 36 in sulfate-reducing incubations stimulated by either acetate, propionate, lactate, or butyrate. In contrast, all methanogenic incubations as well as the sulfate-reducing formate and no-substrate incubations showed, after an initial stimulation until day 8, a steady or even mildly decreasing overall transcriptional activity (Fig. 2b). At day 36, normalized mRNA counts of SbF1 were 56-, 80-, 62-, or 188-fold higher in sulfate-reducing incubations stimulated by either acetate, propionate, lactate, or butyrate, respectively, compared to the no-substrate control and constituted between 0.11 ± 0.13% (acetate) and 0.36 ± 0.02% (butyrate) of all transcripts in the corresponding metatranscriptomes (Fig. 2b). This substrate-specific activity was driven by the increased transcription of genes encoding ribosomal proteins as general activity markers (Fig. 3; Table S1a) and energy metabolism genes, including all canonical dissimilatory sulfate reduction genes (Fig. 4; Table S1a). For example, Spearman's rank correlation coefficients of normalized *dsrA* and *dsrB* transcript counts compared to the sum of normalized SbF1 mRNA counts were 0.91 and 0.90, respectively (FDR-adjusted P value < 0.001). Normalized transcript counts of other enzyme complexes involved in the central metabolism of SbF1, such as the ATP synthase, the NADH dehydrogenase (complex I), and ribosomal proteins, followed the same transcriptional pattern (Fig. 4; Table S1a) with an average Spearman rank correlation coefficient of 0.79 ± 0.07 ($n = 72$, FDR-adjusted P value < 0.05) to the sum of normalized SbF1 mRNA counts. Interestingly, transcription of genes encoding proteins involved in general stress response was stimulated as well. In particular, genes encoding the universal stress promoter UspA, the GroES/GroEL and DnaK chaperons, and the

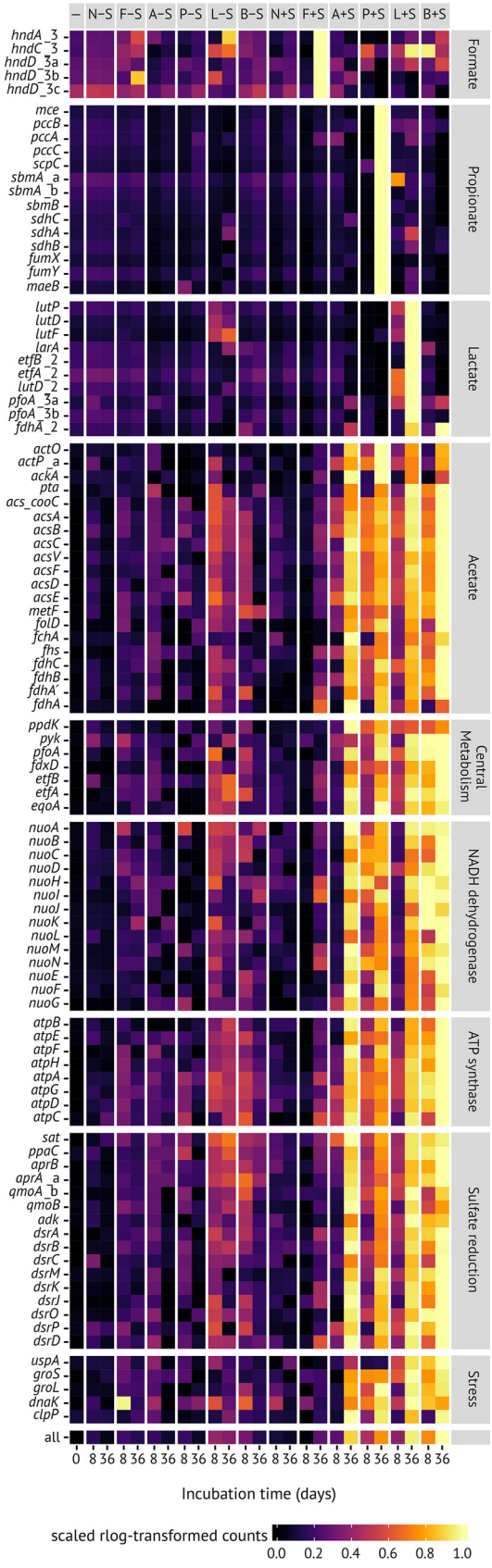

FIG 4 Transcription patterns of whole pathways and central enzyme complexes involved in the carbon and energy metabolism of *Desulfosporosinus* sp. MAG SbF1 under *in situ*-like conditions. In addition,

(Continued on next page)

proteolytic subunit of ATP-dependent Clp protease (ClpP) showed an increased transcription (Fig. 4) with an average Spearman rank correlation coefficient of 0.76 ± 0.04 ($n = 5$, FDR-adjusted P value < 0.05) to the sum of normalized SbF1 mRNA counts. In the microcosms with stimulated transcriptional activity, *dsrA* transcripts of SbF1 constituted also a dominant fraction of overall *dsrA* transcripts ranging from 11% to 53% at day 36 (Fig. S6).

To evaluate whether a hidden turnover of biomass (cryptic growth) was underlying the stable *Desulfosporosinus* population, we screened COG categories D, L, and M for expression of indicator genes that encode functions in cell division (e.g., *ftsZ* or *minE*), DNA replication (e.g., *gyrBA*, *dnaC*, and *dnaG*), and cell envelope biogenesis (e.g., *murABCDEFGI*), respectively. Genes that unambiguously encoded such functions (Table S1a) showed only very minor or no increases in transcripts over time (Fig. 3; detailed in Fig. S5). Extension of this analysis to all genes belonging to COG D ($n = 73$), L ($n = 280$), and M ($n = 215$) showed that the average Spearman rank correlation coefficient to the sum of normalized mRNA counts was only 0.45 ± 0.13 (FDR-adjusted P value < 0.05 [Table S1a]).

We also analyzed genes reported to be upregulated immediately after phage infection, which is an important ecological control of bacterial population size. Respective genes in *Bacillus subtilis* encode, e.g., functions in DNA and protein metabolism and include the ribonucleoside-diphosphate reductase (*nrdEF*) and aspartyl/glutamyl-tRNA amidotransferase (*gatCAB*) (51). However, homologs in SbF1 did not show increased expression in the incubations with increased total transcriptional activity (Table S1a). This was reflected in an average Spearman rank correlation coefficient of only 0.60 ± 0.06 ($n = 4$, FDR-adjusted P value < 0.05) to the sum of normalized SbF1 mRNA counts. The same was true when screening for active sporulation of a *Desulfosporosinus* subpopulation as an alternative explanation for a stable low-abundance population. The identified sporulation genes (*spo0A* to *spoVT*) did not show any prominent increase in transcript numbers as well, with the only exception of *spoIIIAD*, which was stimulated in propionate- and sulfate-amended microcosms (Table S1a). Again, expression of genes involved in sporulation had a low average Spearman rank correlation coefficient of 0.44 ± 0.13 ($n = 22$, FDR-adjusted P value < 0.05) to the sum of normalized SbF1 mRNA counts.

The individual incubation regimes triggered in addition transcriptional activation of the respective substrate degradation pathways of *Desulfosporosinus* sp. MAG SbF1. For example, all genes necessary for the conversion of propionate to pyruvate were overexpressed only upon addition of propionate and sulfate but not in any other incubation type. The same was true for lactate degradation, where genes encoding the lactate permease, lactate racemase, and two of the detected lactate dehydrogenases were overexpressed upon addition of both lactate and sulfate but not in incubations with lactate only (Fig. 4). Although genes encoding phosphotransacetylase and acetate kinase were overexpressed under lactate and propionate, the complete Wood-Ljungdahl pathway was overexpressed as well, which indicates that at least part of these substrates were completely degraded to CO_2 rather than to acetate and CO_2. This conclusion was supported by the overexpression of the Wood-Ljungdahl pathway in incubations amended with acetate and sulfate. Interestingly, the Wood-Ljungdahl pathway was also overexpressed upon addition of butyrate and sulfate. Under such conditions, *Desulfosporosinus* sp. MAG SbF1 apparently relies on acetate released by a butyrate utilizer, as it lacks the capability for butyrate oxidation, albeit failed recovery of the butyrate degradation pathway during binning cannot be excluded.

FIG 4 Legend (Continued)
transcription patterns of general stress response proteins are shown. Mean abundance for the native soil (–) and each incubation treatment and time point is shown. Supplemented substrates are indicated by initials, and addition of external sulfate is depicted by −S/+S (columns). Abundance values are normalized variance-stabilized counts x, which were scaled from 0 to 1 for each CDS using the formula $[x - \min(x)]/\max[x - \min(x)]$. Incompletely assembled genes are indicated by _a, _b, and _c.

DISCUSSION

Current knowledge on the interconnection of energy metabolism, gene expression, cell division, and population growth in microorganisms is mainly based on pure cultures that are maintained in the laboratory. Under ideal conditions, a single *Escherichia coli* cell would grow to a population with the mass of the Earth within 2 days. Clearly, this does not occur, but the discrepancy between potential and actual growth underscores that microorganisms spend the vast majority of their time not dividing (27, 52). A large fraction of these microorganisms are part of the rare biosphere. For example, in the studied peatland, the sum of all low-abundance species made up approximately 12% of the total bacterial and archaeal 16S rRNA genes (5). In other soils, low-abundance *Alphaproteobacteria* and *Bacteroidetes* alone constituted in sum 10% and 9% of the total bacterial population, respectively, while all low-abundance populations summed up to 37% of all bacteria (14). Upon strong environmental change, low-abundance microorganisms often grow to numerically abundant populations and replace dominant species as observed for microbial community changes after an oil spill (53, 54) or in the response of soil microorganisms toward the presence of plants (14). However, subtle environmental changes (5) or recurring seasonal shifts (7, 9, 55) often lead to rather small shifts in low-abundance populations without rare biosphere members becoming numerically dominant.

The low-abundance *Desulfosporosinus* sp. MAG SbF1 represents an interesting case of the latter response type. When exposed to favorable, sulfate-reducing conditions in peat soil microcosms, the overall *Desulfosporosinus* population did not increase its population size of about 1.2×10^6 16S rRNA gene copies cm^{-3} soil (Fig. 2a) but strongly increased its cellular ribosome content by up to 1 order of magnitude (see Fig. S4 in the supplemental material) (5). In a preceding 16S rRNA (gene) amplicon study which analyzed the same microcosms, we could show that *Desulfosporosinus* OTU0051 is the major constituent of this *Desulfosporosinus* population (74% of all *Desulfosporosinus* amplicons) and correlated best in its 16S rRNA response to sulfate turnover among all identified SRM (5). Here, we reanalyzed these microcosms to expand upon this observation by genome-centric metatranscriptomics and to test whether the increase in cellular ribosome content is indeed translated into transcriptional and, as a consequence, metabolic activity. *Desulfosporosinus* OTU0051 was 100% identical to the 16S rRNA gene of *Desulfosporosinus* sp. MAG SbF1, which was retrieved in this study and as such represented the major *Desulfosporosinus* population. In support of this conclusion, increases in 16S rRNA copies of the overall *Desulfosporosinus* population (Fig. S4) (5) clearly corresponded to increased transcription of genes coding for ribosomal proteins in *Desulfosporosinus* sp. MAG SbF1 (Fig. 3; Table S1a) (5). This cellular ribosome increase under sulfate-reducing conditions correlated well with an increase in all normalized mRNA counts (Fig. 2b). This is the first time that changes in population-wide 16S rRNA levels are proven to be directly linked to transcriptional activity for a rare biosphere member.

Analyzing the transcriptional response of a rare biosphere member under *in situ*-like conditions opens the unique opportunity to gain insights into its ecophysiology. *Desulfosporosinus* sp. MAG SbF1 clearly overexpressed its sulfate reduction pathway under sulfate amendment when supplied with either acetate, lactate, propionate, or butyrate compared to the no-substrate and the methanogenic controls (Fig. 4). Here, *dsrA* transcripts of *Desulfosporosinus* sp. MAG SbF1 represented a dominant fraction of all detected *dsrA* transcripts (up to 53%), supporting its importance for the observed sulfate turnover in the analyzed microcosms (Fig. S6). Detailed analysis of the transcribed carbon degradation pathways showed that *Desulfosporosinus* sp. MAG SbF1 is able to oxidize propionate, lactate, and acetate completely to CO_2. This was unexpected, since all described species of the genus *Desulfosporosinus* are so far known as incomplete oxidizers of organic compounds to acetate and CO_2 (56–59). Under butyrate-amended conditions, *Desulfosporosinus* sp. MAG SbF1 presumably relied on uptake of acetate supplied by a primary butyrate oxidizer. This shows that *Desulfospo-*

rosinus sp. MAG SbF1 is capable of utilizing diverse substrates that represent the most important carbon degradation intermediates measured in peatlands (60, 61).

The question remains which mechanisms are at work that keep the transcriptionally active *Desulfosporosinus* sp. MAG SbF1 population in a stable low-abundance state. Ongoing growth could be hidden by continuous predation, viral lysis, or active sporulation of a major subpopulation. To answer this question, we analyzed expression patterns of genes involved in cell growth-associated processes. Compared to the strong overexpression of metabolic or ribosomal protein genes, transcription of genes essential for DNA replication, cell division, and cell envelope biogenesis did not increase or increased only marginally (Fig. 3; Fig. S5). In contrast, retentostat studies on cultured *Firmicutes* held in a (near-) zero-growth state revealed that expression of genes involved in cell growth, central energy metabolism, and the translational apparatus was always coregulated, showing either a joint increased expression in *Bacillus subtilis* (62) or an invariable expression in *Lactobacillus plantarum* (63) when comparing active growth to (near-) zero growth. In addition, there is experimental evidence that in the lag phase of batch cultures, i.e., in the transition from no growth to growth, transcription of growth-related genes is not stable but increases due to the overall activation of cellular processes (64). In this context, the lack of an increasing transcription of growth-related genes would clearly indicate a state of (near-) zero growth rather than an actively dividing population that is kept stable by an equally high growth and mortality or sporulation rate. This conclusion is further supported by the lack of overexpressed sporulation genes or genes upregulated directly after phage attack (Table S1a and c).

Nevertheless, the ATP generated by the induced energy metabolism has to be consumed. If not used for growth, it has to be invested completely for maintenance according to the Herbert-Pirt relation $q_s = m_s + \mu/Y_{sx}^{max}$, where q_s is the biomass-specific consumption rate, m_s is the maintenance coefficient, μ is the specific growth rate, and Y_{sx}^{max} is the maximum growth yield (65, 66). Based on the concept of a species-independent maintenance energy requirement as laid out by reference 67, and further developed by reference 28, it can be calculated that *Desulfosporosinus* sp. MAG SbF1 would need to consume 1.5 fmol sulfate per day to maintain a single cell in our incubations when, e.g., incompletely oxidizing lactate to acetate (detailed in Text S1 in the supplemental material). This is in agreement with experimentally determined maintenance requirements of *Desulfotomaculum putei* (68) but 2 orders of magnitude smaller than the cell-specific sulfate reduction rates of *Desulfosporosinus* sp. MAG SbF1 estimated previously in a similar experimental setup of the same peat soil by reference 16 (here the responsive but low-abundance *Desulfosporosinus* OTU was 99.8% identical to the 16S rRNA gene of *Desulfosporosinus* sp. MAG SbF1). However, maintenance requirements are known to increase upon production of storage compounds or to counterbalance environmental stress (28). We found no indication for the former scenario but observed overexpression of the universal stress promoter UspA, which is one of the most abundant proteins in growth-arrested cells (69). In addition, we observed overexpression of the chaperons GroES/GroEL and DnaK and of the protease ClpP, which were all previously linked to low-pH stress response at the expense of ATP consumption (70–74). Since the pH in the analyzed peat soil incubations varied between 4.1 and 5.0 (5), coping with a low pH would be the most parsimonious explanation for increased maintenance requirements. In this context, one may speculate whether the overexpressed ATP synthase might have operated as an ATPase to pump protons out of the cell at the expense of ATP hydrolysis, which is a known response mechanisms toward mildly acidic pH (74). Similarly, the overexpressed sulfate reduction pathway, including complex I and the membrane quinone shuttle, might have been co-utilized as a proton pump without harvesting the membrane potential for ATP generation. Since active sulfate reduction would also consume protons in the vicinity of *Desulfosporosinus* sp. MAG SbF1 and thus slowly increase its surrounding pH, a high metabolic activity at concomitant zero growth controlled by maintenance requirements would make sense. Favorable conditions lasting longer than the 50 days

studied here may result in increasing the surrounding pH enough for surplus energy to be invested in growth. This would explain the observed abundance increases of *Desulfosporosinus* 16S rRNA genes after 73 days of incubation in a previous study (16) and the detectable ^{13}C incorporation into the genome of the rare peatland *Desulfosporosinus* after 120 days of incubations (increased coverage in the DNA-SIP metagenome). In the context of the dynamic occurrence of sulfate reduction in peatlands, e.g., driven by changes in the water table as the oxic-anoxic interface or the complex flow paths of infiltrating and exfiltrating water that create distinct spatial and temporal activity patterns (47–50), the studied *Desulfosporosinus* population may experience time periods of favorable conditions (as in our incubations) that would result first in activity at zero growth to counteract (pH) stress and, if provided long enough, eventually also in growth.

Our results are important in the context of the increasing awareness that the microbial rare biosphere is not only the largest pool of biodiversity on Earth (1–4) but in sum of all its low-abundance members constitutes also a large part of the biomass in a given habitat (5, 14). Understanding the mechanisms governing this low-abundance prevalence and its direct impact on ecosystem functions and biogeochemical cycling is thus of utmost importance. *Desulfosporosinus* sp. MAG SbF1 has been repeatedly shown to be involved in cryptic sulfur cycling in peatlands (5, 16)—a process that counterbalances the emission of the greenhouse gas methane due to the competitive advantage of SRM compared to microorganisms involved in the methanogenic degradation pathways (20). This species can be found worldwide in low-sulfate environments impacted by cryptic sulfur cycling, including not only peatlands but also permafrost soils, rice paddies, and other wetland types (5). Here, we provided proof that *Desulfosporosinus* sp. MAG SbF1 is indeed involved in the degradation of important anaerobic carbon degradation intermediates in peatlands while sustaining a low-abundance population. It has a generalist lifestyle in respect to the usable carbon sources, re-emphasizing its importance in the carbon and sulfur cycle of peatlands. Our results provide an important step forward in understanding the microbial ecology of biogeochemically relevant microorganisms and show that low-abundance keystone species can be studied "in the wild" using modern environmental systems biology approaches.

Proposal of "*Candidatus* Desulfosporosinus infrequens." Based on its phylogenetic placement and novel ecophysiological behavior, we propose that *Desulfosporosinus* sp. MAG SbF1 represents a novel species with the provisional name "*Candidatus* Desulfosporosinus infrequens" sp. nov. (in.fre'quens. L. adj. *infrequens*, rare, referring to its low relative abundance). Based on its genome-derived metabolic potential and support from metatranscriptomics, "*Ca.* Desulfosporosinus infrequens" is capable of complete oxidation of acetate, propionate, and lactate with sulfate as the electron acceptor, with further potential for oxidation of molecular hydrogen (Fig. 1).

MATERIALS AND METHODS

Genome assembly, binning, and phylogenetic inference. Sampling of peat soil from the acidic peatland Schlöppnerbrunnen II (Germany), DNA-stable isotope probing (DNA-SIP), total nucleic acid extraction, metagenome sequencing and assembly, and coverage-based binning were described previously (5, 16, 29). In brief, DNA from native peat soil (10- to 20-cm depth) and DNA pooled from 16 ^{13}C-enriched fractions (density, 1.715 to 1.726 g ml^{-1}) of a previous DNA-SIP experiment with soil from the same site (16) was sequenced using the Illumina HiSeq 2000 system. DNA-SIP was performed after a 120-day incubation (again, 10- to 20-cm depth) that was periodically amended with small dosages of sulfate and first a mixture of unlabeled formate, acetate, propionate, and lactate for 2 weeks and thereafter a mixture of ^{13}C-labeled formate, acetate, propionate, and lactate (all in the lower-micromolar range) (16). Raw reads were quality filtered, trimmed, and coassembled (native soil, 385 million reads; DNA-SIP, 576 million reads) using the CLC Genomics Workbench 5.5.1 (CLC Bio). Differential coverage binning was applied to extract the *Desulfosporosinus* metagenome-assembled genome (MAG) (75). As expected (16), the *Desulfosporosinus* MAG was of low abundance in the native soil with an average coverage of 0.026 while enriched in the SIP sample with an average coverage of 34 (detailed per scaffold in Table S1b). A side effect of sequencing a DNA-SIP sample is an apparent G+C content skew, which was normalized arbitrarily to improve binning using the following formula (29, 76): $(\text{coverage}/G+C\ \text{content}^9) \times 10^{15}$.

Scaffolds containing the 16S and 23S rRNA genes were successfully identified using paired-end linkage data (75). Completeness, contamination, and strain heterogeneity were estimated using CheckM 1.0.6 (77).

Phylogenomic analysis of the *Desulfosporosinus* MAG was based on a concatenated set of 34 phylogenetically informative marker genes as defined by reference 77 and the Bayesian phylogeny inference method PhyloBayes using the CAT-GTR model (78). 16S rRNA gene-based phylogeny was inferred using the ARB SILVA database r126 as a reference (79), the SINA aligner (80), and the substitution model testing and maximum likelihood treeing method IQ-TREE (81). Pairwise 16S rRNA gene sequence identities were calculated with T-Coffee 11 (82). Pairwise average nucleic and amino acid identities (ANI and AAI, respectively) (37) between protein-encoding genes of the *Desulfosporosinus* MAG and reference genomes were calculated as described previously (29).

Genome annotation. The genome was annotated using the MicroScope annotation platform (83). Annotation refinement for selected genes was done as follows: proteins with an amino acid identity ≥40% (over ≥80% of the sequence) to a Swiss-Prot entry (84) or a curated MaGe annotation (83) or proteins described in the literature were annotated as true homologs of known proteins. The same was true if classification according to InterPro families (85, 86), TIGRFAMs (87), and/or FIGfams (88) led to an unambiguous annotation. Proteins with an amino acid identity ≥25% (over ≥80% of the sequence) to a Swiss-Prot or TrEMBL (84) entry were annotated as putative homologs of the respective database entries. In addition, classification according to COG (89) or InterPro superfamilies, domains, or binding sites was used to call putative homologs in cases of an unambiguous annotation. Membership to syntenic regions (operons) was considered additional support to call true or putative homologs.

Metatranscriptomics from single-substrate incubations. Metatranscriptomic data sets of anoxic peat soil slurry microcosms that were previously described (29) were re-analyzed in the context of published *Desulfosporosinus* qPCR data (5) of the same microcosms. In brief, anoxic microcosms were incubated at 14°C in the dark for 50 days and regularly either amended with small amounts of sulfate (76 to 387 μM final concentrations) or incubated without an external electron acceptor. Formate, acetate, propionate, lactate, butyrate (<200 μM), or no external electron donor was added to biological triplicates each. DNA and/or RNA wase extracted from the native soil and after 5, 8, 15, 26, 36, and 50 days of incubations. Quantitative PCR data describing 16S rRNA gene copies of the complete *Desulfosporosinus* population (three species-level operational taxonomic units [OTUs]: 74% OTU0051, 26% OTU0228, and <0.001% OTU7382; average of the native peat soil and all microcosms) in comparison to the overall bacterial and archaeal community were taken from reference 5 and used in this study to put the metatranscriptome data into the perspective of population dynamics. PCR conditions are given in reference 5. Metatranscriptome sequencing was done from each of the biological replicates using the Illumina HiSeq 2000/2500 platform (27 to 188 million reads per sample). Raw reads were quality filtered as described previously (29) and mapped to the *Desulfosporosinus* MAG in a background of all other metagenome-assembled scaffolds using Bowtie 2 at default settings (90). Counting of mapped reads to protein-encoding genes (CDS) was performed with featureCounts 1.5.0 (91).

Statistical analysis of *Desulfosporosinus*-specific transcripts. Counts of mapped transcript reads were normalized to the length of the respective gene and the sequencing depth of the respective metatranscriptome, resulting in FPKM (fragments per kilobase per million total fragments) values. Thereafter, we used an unsupervised approach to identify CDS expression stimulated by sulfate and the different substrates regimes. First, we applied the DESeq2 R package (92, 93) to identify differentially expressed CDS. Treatments without external sulfate added and samples after 8 days of incubations had too few transcript counts to be used for a statistical approach. Therefore, we limited our analysis to pairwise comparison of sulfate-stimulated microcosms after 36 days of incubation. We compared each substrate regime to the no-substrate controls and each other. The set of all significantly differentially expressed CDS (FDR-adjusted P value < 0.05) was further clustered into response groups. For clustering, we calculated pairwise Pearson correlation coefficients (r) of variance stabilized counts (cor function in R) and transformed this into distances ($1 - r$), followed by hierarchical clustering (hclust function in R). Variance stabilization was performed using the rlog function of the DESeq2 package. Spearman's rank correlation of FPKM values for each gene to the total relative mRNA counts was performed with cor.test in R using the data from all treatments and replicates.

Sequence data availability. The MAG SbF1 is available at MicroScope (https://www.genoscope.cns.fr/agc/microscope/) and is also deposited under the GenBank accession number OMOF01000000. Metagenome and transcriptomic data are available at the Joint Genome Institute (https://genome.jgi.doe.gov/) and are also deposited under the GenBank accession numbers PRJNA412436 and PRJNA412438, respectively.

SUPPLEMENTAL MATERIAL

Supplemental material for this article may be found at https://doi.org/10.1128/mBio.02189-18.

TEXT S1, PDF file, 0.2 MB.
FIG S1, PDF file, 1.3 MB.
FIG S2, PDF file, 0.1 MB.
FIG S3, PDF file, 0.04 MB.
FIG S4, PDF file, 0.02 MB.
FIG S5, PDF file, 0.1 MB.

FIG S6, PDF file, 0.03 MB.
TABLE S1, XLSX file, 1.7 MB.

ACKNOWLEDGMENTS

We are grateful to Mads Albertsen, Norbert Bittner, Tijana Glavina del Rio, Florian Goldenberg, Craig Herbold, Stephan Köstlbacher, Per H. Nielsen, Ulrich Stingl, and Susannah G. Tringe for sequence analysis and technical support. We further thank Bernhard Schink for help in naming "*Ca.* Desulfosporosinus infrequens"; Kenneth Wasmund for valuable feedback; and Johannes Wittmann, Jan-Ulrich Kreft, and Silvia Bulgheresi for helpful expert opinions.

We acknowledge the LABGeM (CEA/IG/Genoscope and& CNRS UMR8030) and the France Génomique National infrastructure (funded as part of Investissement d'avenir program managed by Agence Nationale pour la Recherche, contract ANR-10-INBS-09) for support with the MicroScope annotation platform. The work conducted by the Joint Genome Institute was supported by the Office of Science of the U.S. Department of Energy under contract no. DE-AC02-05CH11231. This research was financially supported by the Austrian Science Fund (FWF, P23117-B17 to M.P. and A.L. and P25111-B22 to A.L.), the U.S. Department of Energy (CSP605 to M.P. and A.L.), the German Research Foundation (DFG, PE 2147/1-1 to M.P.), and the European Union (FP7-People-2013-CIG, grant no. PCIG14-GA-2013-630188 to M.P.).

The authors declare no conflict of interest.

REFERENCES

1. Sogin ML, Morrison HG, Huber JA, Mark Welch D, Huse SM, Neal PR, Arrieta JM, Herndl GJ. 2006. Microbial diversity in the deep sea and the underexplored rare biosphere. Proc Natl Acad Sci U S A 103:12115–12120. https://doi.org/10.1073/pnas.0605127103.
2. Pedrós-Alió C. 2012. The rare bacterial biosphere. Annu Rev Mar Sci 4:449–466. https://doi.org/10.1146/annurev-marine-120710-100948.
3. Lynch MDJ, Neufeld JD. 2015. Ecology and exploration of the rare biosphere. Nat Rev Microbiol 13:217–229. https://doi.org/10.1038/nrmicro3400.
4. Jousset A, Bienhold C, Chatzinotas A, Gallien L, Gobet A, Kurm V, Küsel K, Rillig MC, Rivett DW, Salles JF, van der Heijden MGA, Youssef NH, Zhang X, Wei Z, Hol WHG. 2017. Where less may be more: how the rare biosphere pulls ecosystems strings. ISME J 11:853–862. https://doi.org/10.1038/ismej.2016.174.
5. Hausmann B, Knorr K-H, Schreck K, Tringe SG, Glavina del Rio T, Loy A, Pester M. 2016. Consortia of low-abundance bacteria drive sulfate reduction-dependent degradation of fermentation products in peat soil microcosms. ISME J 10:2365–2375. https://doi.org/10.1038/ismej.2016.42.
6. Müller AL, de Rezende JR, Hubert CRJ, Kjeldsen KU, Lagkouvardos I, Berry D, Jørgensen BB, Loy A. 2014. Endospores of thermophilic bacteria as tracers of microbial dispersal by ocean currents. ISME J 8:1153–1165. https://doi.org/10.1038/ismej.2013.225.
7. Campbell BJ, Yu L, Heidelberg JF, Kirchman DL. 2011. Activity of abundant and rare bacteria in a coastal ocean. Proc Natl Acad Sci U S A 108:12776–12781. https://doi.org/10.1073/pnas.1101405108.
8. Hugoni M, Taib N, Debroas D, Domaizon I, Jouan Dufournel I, Bronner G, Salter I, Agogué H, Mary I, Galand PE. 2013. Structure of the rare archaeal biosphere and seasonal dynamics of active ecotypes in surface coastal waters. Proc Natl Acad Sci U S A 110:6004–6009. https://doi.org/10.1073/pnas.1216863110.
9. Alonso-Sáez L, Díaz-Pérez L, Morán XAG. 2015. The hidden seasonality of the rare biosphere in coastal marine bacterioplankton. Environ Microbiol 17:3766–3780. https://doi.org/10.1111/1462-2920.12801.
10. van Elsas JD, Chiurazzi M, Mallon CA, Elhottova D, Kristufek V, Salles JF. 2012. Microbial diversity determines the invasion of soil by a bacterial pathogen. Proc Natl Acad Sci U S A 109:1159–1164. https://doi.org/10.1073/pnas.1109326109.
11. Vivant A-L, Garmyn D, Maron P-A, Nowak V, Piveteau P. 2013. Microbial diversity and structure are drivers of the biological barrier effect against Listeria monocytogenes in soil. PLoS One 8:e76991. https://doi.org/10.1371/journal.pone.0076991.
12. Mallon CA, Poly F, Le Roux X, Marring I, van Elsas JD, Salles JF. 2015. Resource pulses can alleviate the biodiversity-invasion relationship in soil microbial communities. Ecology 96:915–926. https://doi.org/10.1890/14-1001.1.
13. Hol WHG, Garbeva P, Hordijk C, Hundscheid PJ, Gunnewiek PJAK, Van Agtmaal M, Kuramae EE, De Boer W. 2015. Non-random species loss in bacterial communities reduces antifungal volatile production. Ecology 96:2042–2048. https://doi.org/10.1890/14-2359.1.
14. Dawson W, Hör J, Egert M, van KM, Pester M. 2017. A small number of low-abundance bacteria dominate plant species-specific responses during rhizosphere colonization. Front Microbiol 8:975. https://doi.org/10.3389/fmicb.2017.00975.
15. Großkopf T, Mohr W, Baustian T, Schunck H, Gill D, Kuypers MMM, Lavik G, Schmitz RA, Wallace DWR, LaRoche J. 2012. Doubling of marine dinitrogen-fixation rates based on direct measurements. Nature 488:361–364. https://doi.org/10.1038/nature11338.
16. Pester M, Bittner N, Deevong P, Wagner M, Loy A. 2010. A 'rare biosphere' microorganism contributes to sulfate reduction in a peatland. ISME J 4:1591–1602. https://doi.org/10.1038/ismej.2010.75.
17. Pester M, Knorr K-H, Friedrich MW, Wagner M, Loy A. 2012. Sulfate-reducing microorganisms in wetlands—fameless actors in carbon cycling and climate change. Front Microbiol 3:72. https://doi.org/10.3389/fmicb.2012.00072.
18. Jørgensen BB. 1982. Mineralization of organic matter in the sea bed—the role of sulphate reduction. Nature 296:643–645. https://doi.org/10.1038/296643a0.
19. Bowles MW, Mogollón JM, Kasten S, Zabel M, Hinrichs K-U. 2014. Global rates of marine sulfate reduction and implications for sub-sea-floor metabolic activities. Science 344:889–891. https://doi.org/10.1126/science.1249213.
20. Muyzer G, Stams AJM. 2008. The ecology and biotechnology of sulphate-reducing bacteria. Nat Rev Microbiol 6:441–454. https://doi.org/10.1038/nrmicro1892.
21. Gauci V, Matthews E, Dise N, Walter B, Koch D, Granberg G, Vile M. 2004. Sulfur pollution suppression of the wetland methane source in the 20th and 21st centuries. Proc Natl Acad Sci U S A 101:12583–12587. https://doi.org/10.1073/pnas.0404412101.
22. Gauci V, Dise N, Blake S. 2005. Long-term suppression of wetland methane flux following a pulse of simulated acid rain. Geophys Res Lett 32:L12804.
23. Gauci V, Chapman SJ. 2006. Simultaneous inhibition of CH_4 efflux and stimulation of sulphate reduction in peat subject to simulated acid rain.

Soil Biol Biochem 38:3506–3510. https://doi.org/10.1016/j.soilbio.2006.05.011.
24. Ciais P, Sabine C, Bala G, Bopp L, Brovkin V, Canadell J, Chhabra A, DeFries R, Galloway J, Heimann M, Jones C, Quéré CL, Myneni R, Piao S, Thornton P. 2013. Carbon and other biogeochemical cycles. *In* Stocker T, Qin D, Plattner G-K, Tignor M, Allen S, Boschung J, Nauels A, Xia Y, Bex V, Midgley P (ed), Climate change 2013. The physical science basis. Cambridge University Press, Cambridge, United Kingdom.
25. Kirschke S, Bousquet P, Ciais P, Saunois M, Canadell JG, Dlugokencky EJ, Bergamaschi P, Bergmann D, Blake DR, Bruhwiler L, Cameron-Smith P, Castaldi S, Chevallier F, Feng L, Fraser A, Heimann M, Hodson EL, Houweling S, Josse B, Fraser PJ, Krummel PB, Lamarque J-F, Langenfelds RL, Le Quéré C, Naik V, O'Doherty S, Palmer PI, Pison I, Plummer D, Poulter B, Prinn RG, Rigby M, Ringeval B, Santini M, Schmidt M, Shindell DT, Simpson IJ, Spahni R, Steele LP, Strode SA, Sudo K, Szopa S, van der Werf GR, Voulgarakis A, van Weele M, Weiss RF, Williams JE, Zeng G. 2013. Three decades of global methane sources and sinks. Nat Geosci 6:813–823. https://doi.org/10.1038/ngeo1955.
26. Saunois M, Bousquet P, Poulter B, Peregon A, Ciais P, Canadell JG, Dlugokencky EJ, Etiope G, Bastviken D, Houweling S, Janssens-Maenhout G, Tubiello FN, Castaldi S, Jackson RB, Alexe M, Arora VK, Beerling DJ, Bergamaschi P, Blake DR, Brailsford G, Brovkin V, Bruhwiler L, Crevoisier C, Crill P, Covey K, Curry C, Frankenberg C, Gedney N, Höglund-Isaksson L, Ishizawa M, Ito A, Joos F, Kim H-S, Kleinen T, Krummel P, Lamarque J-F, Langenfelds R, Locatelli R, Machida T, Maksyutov S, McDonald KC, Marshall J, Melton JR, Morino I, Naik V, O'Doherty S, Parmentier F-JW, Patra PK, Peng C, Peng S, Peters GP, Pison I, Prigent C, Prinn R, Ramonet M, Riley WJ, Saito M, Santini M, Schroeder R, Simpson IJ, Spahni R, Steele P, Takizawa A, Thornton BF, Tian H, Tohjima Y, Viovy N, Voulgarakis A, van Weele M, van der Werf GR, Weiss R, Wiedinmyer C, Wilton DJ, Wiltshire A, Worthy D, Wunch D, Xu X, Yoshida Y, Zhang B, Zhang Z, Zhu Q. 2016. The global methane budget 2000–2012. Earth Syst Sci Data 8:697–751.
27. Lever MA, Rogers KL, Lloyd KG, Overmann J, Schink B, Thauer RK, Hoehler TM, Jørgensen BB. 2015. Life under extreme energy limitation: a synthesis of laboratory- and field-based investigations. FEMS Microbiol Rev 39:688–728. https://doi.org/10.1093/femsre/fuv020.
28. Harder J. 2006. Species-independent maintenance energy and natural population sizes. FEMS Microbiol Ecol 23:39–44. https://doi.org/10.1111/j.1574-6941.1997.tb00389.x.
29. Hausmann B, Pelikan C, Herbold CW, Köstlbacher S, Albertsen M, Eichorst SA, Glavina Del Rio T, Huemer M, Nielsen PH, Rattei T, Stingl U, Tringe SG, Trojan D, Wentrup C, Woebken D, Pester M, Loy A. 2018. Peatland *Acidobacteria* with a dissimilatory sulfur metabolism. ISME J 12:1729–1742. https://doi.org/10.1038/s41396-018-0077-1.
30. Abicht HK, Mancini S, Karnachuk OV, Solioz M. 2011. Genome sequence of *Desulfosporosinus* sp. OT, an acidophilic sulfate-reducing bacterium from copper mining waste in Norilsk, Northern Siberia. J Bacteriol 193:6104–6105. https://doi.org/10.1128/JB.06018-11.
31. Pester M, Brambilla E, Alazard D, Rattei T, Weinmaier T, Han J, Lucas S, Lapidus A, Cheng J-F, Goodwin L, Pitluck S, Peters L, Ovchinnikova G, Teshima H, Detter JC, Han CS, Tapia R, Land ML, Hauser L, Kyrpides NC, Ivanova NN, Pagani I, Huntmann M, Wei C-L, Davenport KW, Daligault H, Chain PSG, Chen A, Mavromatis K, Markowitz V, Szeto E, Mikhailova N, Pati A, Wagner M, Woyke T, Ollivier B, Klenk H-P, Spring S, Loy A. 2012. Complete genome sequences of *Desulfosporosinus orientis* DSM765^T, *Desulfosporosinus youngiae* DSM17734^T, *Desulfosporosinus meridiei* DSM13257^T, and *Desulfosporosinus acidiphilus* DSM22704^T. J Bacteriol 194:6300–6301. https://doi.org/10.1128/JB.01392-12.
32. Abu Laban N, Tan B, Dao A, Foght J. 2015. Draft genome sequence of uncultivated *Desulfosporosinus* sp. strain Tol-M, obtained by stable isotope probing using [$^{13}C_6$]toluene. Genome Announc 3:e01422-14. https://doi.org/10.1128/genomeA.01422-14.
33. Petzsch P, Poehlein A, Johnson DB, Daniel R, Schlömann M, Mühling M. 2015. Genome sequence of the moderately acidophilic sulfate-reducing firmicute *Desulfosporosinus acididurans* (strain M1^T). Genome Announc 3:e00881-15. https://doi.org/10.1128/genomeA.00881-15.
34. Mardanov AV, Panova IA, Beletsky AV, Avakyan MR, Kadnikov VV, Antsiferov DV, Banks D, Frank YA, Pimenov NV, Ravin NV, Karnachuk OV. 2016. Genomic insights into a new acidophilic, copper-resistant *Desulfosporosinus* isolate from the oxidized tailings area of an abandoned gold mine. FEMS Microbiol Ecol 92:fiw111. https://doi.org/10.1093/femsec/fiw111.
35. Stoddard SF, Smith BJ, Hein R, Roller BRK, Schmidt TM. 2015. *rrn*DB: improved tools for interpreting rRNA gene abundance in bacteria and archaea and a new foundation for future development. Nucleic Acids Res 43:D593–D598. https://doi.org/10.1093/nar/gku1201.
36. Stackebrandt E, Ebers J. 2006. Taxonomic parameters revisited: tarnished gold standards. Microbiol Today 33:152–155.
37. Varghese NJ, Mukherjee S, Ivanova N, Konstantinidis KT, Mavrommatis K, Kyrpides NC, Pati A. 2015. Microbial species delineation using whole genome sequences. Nucleic Acids Res 43:6761–6771. https://doi.org/10.1093/nar/gkv657.
38. Rabus R, Venceslau SS, Wöhlbrand L, Voordouw G, Wall JD, Pereira IAC. 2015. A post-genomic view of the ecophysiology, catabolism and biotechnological relevance of sulphate-reducing prokaryotes. Adv Microb Physiol 66:55–321. https://doi.org/10.1016/bs.ampbs.2015.05.002.
39. Huang CJ, Barrett EL. 1991. Sequence analysis and expression of the *Salmonella typhimurium asr* operon encoding production of hydrogen sulfide from sulfite. J Bacteriol 173:1544–1553.
40. Weghoff MC, Bertsch J, Müller V. 2015. A novel mode of lactate metabolism in strictly anaerobic bacteria. Environ Microbiol 17:670–677. https://doi.org/10.1111/1462-2920.12493.
41. Zhang Y, Jiang T, Sheng B, Long Y, Gao C, Ma C, Xu P. 2016. Coexistence of two D-lactate-utilizing systems in *Pseudomonas putida* KT2440. Environ Microbiol Rep 8:699–707. https://doi.org/10.1111/1758-2229.12429.
42. Desguin B, Goffin P, Viaene E, Kleerebezem M, Martin-Diaconescu V, Maroney MJ, Declercq J-P, Soumillion P, Hols P. 2014. Lactate racemase is a nickel-dependent enzyme activated by a widespread maturation system. Nat Commun 5:3615. https://doi.org/10.1038/ncomms4615.
43. Pierce E, Xie G, Barabote RD, Saunders E, Han CS, Detter JC, Richardson P, Brettin TS, Das A, Ljungdahl LG, Ragsdale SW. 2008. The complete genome sequence of *Moorella thermoacetica* (f. *Clostridium thermoaceticum*). Environ Microbiol 10:2550–2573. https://doi.org/10.1111/j.1462-2920.2008.01679.x.
44. Greening C, Biswas A, Carere CR, Jackson CJ, Taylor MC, Stott MB, Cook GM, Morales SE. 2016. Genomic and metagenomic surveys of hydrogenase distribution indicate H_2 is a widely utilised energy source for microbial growth and survival. ISME J 10:761–777. https://doi.org/10.1038/ismej.2015.153.
45. Schmidt A, Müller N, Schink B, Schleheck D. 2013. A proteomic view at the biochemistry of syntrophic butyrate oxidation in *Syntrophomonas wolfei*. PLoS One 8:e56905. https://doi.org/10.1371/journal.pone.0056905.
46. Buckel W, Thauer RK. 2013. Energy conservation via electron bifurcating ferredoxin reduction and proton/Na^+ translocating ferredoxin oxidation. Biochim Biophys Acta 1827:94–113. https://doi.org/10.1016/j.bbabio.2012.07.002.
47. Jacks G, Norrström A-C. 2004. Hydrochemistry and hydrology of forest riparian wetlands. For Ecol Manage 196:187–197. https://doi.org/10.1016/j.foreco.2004.01.055.
48. Knorr K-H, Lischeid G, Blodau C. 2009. Dynamics of redox processes in a minerotrophic fen exposed to a water table manipulation. Geoderma 153:379–392. https://doi.org/10.1016/j.geoderma.2009.08.023.
49. Knorr K-H, Blodau C. 2009. Impact of experimental drought and rewetting on redox transformations and methanogenesis in mesocosms of a northern fen soil. Soil Biol Biochem 41:1187–1198. https://doi.org/10.1016/j.soilbio.2009.02.030.
50. Frei S, Knorr K-H, Peiffer S, Fleckenstein JH. 2012. Surface microtopography causes hot spots of biogeochemical activity in wetland systems: a virtual modeling experiment. J Geophys Res Biogeosci 117:G00N12.
51. Mojardín L, Salas M. 2016. Global transcriptional analysis of virus-host interactions between phage ϕ29 and *Bacillus subtilis*. J Virol 90:9293–9304. https://doi.org/10.1128/JVI.01245-16.
52. Bergkessel M, Basta DW, Newman DK. 2016. The physiology of growth arrest: uniting molecular and environmental microbiology. Nat Rev Microbiol 14:549–562. https://doi.org/10.1038/nrmicro.2016.107.
53. Teira E, Lekunberri I, Gasol JM, Nieto-Cid M, Alvarez-Salgado XA, Figueiras FG. 2007. Dynamics of the hydrocarbon-degrading *Cycloclasticus* bacteria during mesocosm-simulated oil spills. Environ Microbiol 9:2551–2562. https://doi.org/10.1111/j.1462-2920.2007.01373.x.
54. Newton RJ, Huse SM, Morrison HG, Peake CS, Sogin ML, McLellan SL. 2013. Shifts in the microbial community composition of Gulf Coast beaches following beach oiling. PLoS One 8:e74265. https://doi.org/10.1371/journal.pone.0074265.
55. Vergin K, Done B, Carlson C, Giovannoni S. 2013. Spatiotemporal distributions of rare bacterioplankton populations indicate adaptive strate-

gies in the oligotrophic ocean. Aquat Microb Ecol 71:1–13. https://doi.org/10.3354/ame01661.
56. Alazard D, Joseph M, Battaglia-Brunet F, Cayol J-L, Ollivier B. 2010. *Desulfosporosinus acidiphilus* sp. nov.: a moderately acidophilic sulfate-reducing bacterium isolated from acid mining drainage sediments. Extremophiles 14:305–312. https://doi.org/10.1007/s00792-010-0309-4.
57. Mayeux B, Fardeau M-L, Bartoli-Joseph M, Casalot L, Vinsot A, Labat M. 2013. *Desulfosporosinus burensis* sp. nov., a spore-forming, mesophilic, sulfate-reducing bacterium isolated from a deep clay environment. Int J Syst Evol Microbiol 63:593–598. https://doi.org/10.1099/ijs.0.035238-0.
58. Sánchez-Andrea I, Stams AJM, Hedrich S, Ñancucheo I, Johnson DB. 2015. *Desulfosporosinus acididurans* sp. nov.: an acidophilic sulfate-reducing bacterium isolated from acidic sediments. Extremophiles 19:39–47. https://doi.org/10.1007/s00792-014-0701-6.
59. Vandieken V, Niemann H, Engelen B, Cypionka H. 2017. *Marinisporobacter balticus* gen. nov., sp. nov., *Desulfosporosinus nitroreducens* sp. nov. and *Desulfosporosinus fructosivorans* sp. nov., new spore-forming bacteria isolated from subsurface sediments of the Baltic Sea. Int J Syst Evol Microbiol 67:1887–1893. https://doi.org/10.1099/ijsem.0.001883.
60. Schmalenberger A, Drake HL, Küsel K. 2007. High unique diversity of sulfate-reducing prokaryotes characterized in a depth gradient in an acidic fen. Environ Microbiol 9:1317–1328. https://doi.org/10.1111/j.1462-2920.2007.01251.x.
61. Küsel K, Blöthe M, Schulz D, Reiche M, Drake HL. 2008. Microbial reduction of iron and porewater biogeochemistry in acidic peatlands. Biogeosciences 5:1537–1549. https://doi.org/10.5194/bg-5-1537-2008.
62. Overkamp W, Ercan O, Herber M, van Maris AJA, Kleerebezem M, Kuipers OP. 2015. Physiological and cell morphology adaptation of *Bacillus subtilis* at near-zero specific growth rates: a transcriptome analysis. Environ Microbiol 17:346–363. https://doi.org/10.1111/1462-2920.12676.
63. Goffin P, van de Bunt B, Giovane M, Leveau JHJ, Höppener-Ogawa S, Teusink B, Hugenholtz J. 2010. Understanding the physiology of *Lactobacillus plantarum* at zero growth. Mol Syst Biol 6:413. https://doi.org/10.1038/msb.2010.67.
64. Rolfe MD, Rice CJ, Lucchini S, Pin C, Thompson A, Cameron ADS, Alston M, Stringer MF, Betts RP, Baranyi J, Peck MW, Hinton JCD. 2012. Lag phase is a distinct growth phase that prepares bacteria for exponential growth and involves transient metal accumulation. J Bacteriol 194:686–701. https://doi.org/10.1128/JB.06112-11.
65. Pirt SJ. 1965. The maintenance energy of bacteria in growing cultures. Proc R Soc Lond B Biol Sci 163:224–231. https://doi.org/10.1098/rspb.1965.0069.
66. Ercan O, Bisschops MMM, Overkamp W, Jørgensen TR, Ram AF, Smid EJ, Pronk JT, Kuipers OP, Daran-Lapujade P, Kleerebezem M. 2015. Physiological and transcriptional responses of different industrial microbes at near-zero specific growth rates. Appl Environ Microbiol 81:5662–5670. https://doi.org/10.1128/AEM.00944-15.
67. Tijhuis L, Van Loosdrecht MC, Heijnen JJ. 1993. A thermodynamically based correlation for maintenance gibbs energy requirements in aerobic and anaerobic chemotrophic growth. Biotechnol Bioeng 42:509–519. https://doi.org/10.1002/bit.260420415.
68. Davidson MM, Bisher ME, Pratt LM, Fong J, Southam G, Pfiffner SM, Reches Z, Onstott TC. 2009. Sulfur isotope enrichment during maintenance metabolism in the thermophilic sulfate-reducing bacterium *Desulfotomaculum putei*. Appl Environ Microbiol 75:5621–5630. https://doi.org/10.1128/AEM.02948-08.
69. Kvint K, Nachin L, Diez A, Nyström T. 2003. The bacterial universal stress protein: function and regulation. Curr Opin Microbiol 6:140–145.
70. Jan G, Leverrier P, Pichereau V, Boyaval P. 2001. Changes in protein synthesis and morphology during acid adaptation of *Propionibacterium freudenreichii*. Appl Environ Microbiol 67:2029–2036. https://doi.org/10.1128/AEM.67.5.2029-2036.2001.
71. Frees D, Vogensen FK, Ingmer H. 2003. Identification of proteins induced at low pH in *Lactococcus lactis*. Int J Food Microbiol 87:293–300.
72. Sánchez B, Champomier-Vergès M-C, Collado MDC, Anglade P, Baraige F, Sanz Y, de los Reyes-Gavilán CG, Margolles A, Zagorec M. 2007. Low-pH adaptation and the acid tolerance response of *Bifidobacterium longum* biotype longum. Appl Environ Microbiol 73:6450–6459. https://doi.org/10.1128/AEM.00886-07.
73. Silva J, Carvalho AS, Ferreira R, Vitorino R, Amado F, Domingues P, Teixeira P, Gibbs PA. 2005. Effect of the pH of growth on the survival of *Lactobacillus delbrueckii* subsp. *bulgaricus* to stress conditions during spray-drying. J Appl Microbiol 98:775–782. https://doi.org/10.1111/j.1365-2672.2004.02516.x.
74. Lund P, Tramonti A, De Biase D. 2014. Coping with low pH: molecular strategies in neutralophilic bacteria. FEMS Microbiol Rev 38:1091–1125. https://doi.org/10.1111/1574-6976.12076.
75. Albertsen M, Hugenholtz P, Skarshewski A, Nielsen KL, Tyson GW, Nielsen PH. 2013. Genome sequences of rare, uncultured bacteria obtained by differential coverage binning of multiple metagenomes. Nat Biotechnol 31:533–538. https://doi.org/10.1038/nbt.2579.
76. Herbold CW, Lehtovirta-Morley LE, Jung M-Y, Jehmlich N, Hausmann B, Han P, Loy A, Pester M, Sayavedra-Soto LA, Rhee S-K, Prosser JI, Nicol GW, Wagner M, Gubry-Rangin C. 2017. Ammonia-oxidising archaea living at low pH: insights from comparative genomics. Environ Microbiol 19:4939–4952. https://doi.org/10.1111/1462-2920.13971.
77. Parks DH, Imelfort M, Skennerton CT, Hugenholtz P, Tyson GW. 2015. CheckM: assessing the quality of microbial genomes recovered from isolates, single cells, and metagenomes. Genome Res 25:1043–1055. https://doi.org/10.1101/gr.186072.114.
78. Lartillot N, Lepage T, Blanquart S. 2009. PhyloBayes 3: a Bayesian software package for phylogenetic reconstruction and molecular dating. Bioinformatics 25:2286–2288. https://doi.org/10.1093/bioinformatics/btp368.
79. Quast C, Pruesse E, Yilmaz P, Gerken J, Schweer T, Yarza P, Peplies J, Glöckner FO. 2012. The SILVA ribosomal RNA gene database project: improved data processing and web-based tools. Nucleic Acids Res 41:D590–D596. https://doi.org/10.1093/nar/gks1219.
80. Pruesse E, Peplies J, Glöckner FO. 2012. SINA: accurate high-throughput multiple sequence alignment of ribosomal RNA genes. Bioinformatics 28:1823–1829. https://doi.org/10.1093/bioinformatics/bts252.
81. Trifinopoulos J, Nguyen L-T, von Haeseler A, Minh BQ. 2016. W-IQ-TREE: a fast online phylogenetic tool for maximum likelihood analysis. Nucleic Acids Res 44:W232–W235. https://doi.org/10.1093/nar/gkw256.
82. Notredame C, Higgins DG, Heringa J. 2000. T-Coffee: a novel method for fast and accurate multiple sequence alignment. J Mol Biol 302:205–217. https://doi.org/10.1006/jmbi.2000.4042.
83. Vallenet D, Calteau A, Cruveiller S, Gachet M, Lajus A, Josso A, Mercier J, Renaux A, Rollin J, Rouy Z, Roche D, Scarpelli C, Médigue C. 2017. MicroScope in 2017: an expanding and evolving integrated resource for community expertise of microbial genomes. Nucleic Acids Res 45:D517–D528. https://doi.org/10.1093/nar/gkw1101.
84. The UniProt Consortium. 2017. UniProt: the universal protein knowledgebase. Nucleic Acids Res 45:D158–D169. https://doi.org/10.1093/nar/gkw1099.
85. Mitchell A, Chang H-Y, Daugherty L, Fraser M, Hunter S, Lopez R, McAnulla C, McMenamin C, Nuka G, Pesseat S, Sangrador-Vegas A, Scheremetjew M, Rato C, Yong S-Y, Bateman A, Punta M, Attwood TK, Sigrist CJA, Redaschi N, Rivoire C, Xenarios I, Kahn D, Guyot D, Bork P, Letunic I, Gough J, Oates M, Haft D, Huang H, Natale DA, Wu CH, Orengo C, Sillitoe I, Mi H, Thomas PD, Finn RD. 2015. The InterPro protein families database: the classification resource after 15 years. Nucleic Acids Res 43:D213–D221. https://doi.org/10.1093/nar/gku1243.
86. Jones P, Binns D, Chang H-Y, Fraser M, Li W, McAnulla C, McWilliam H, Maslen J, Mitchell A, Nuka G, Pesseat S, Quinn AF, Sangrador-Vegas A, Scheremetjew M, Yong S-Y, Lopez R, Hunter S. 2014. InterProScan 5: genome-scale protein function classification. Bioinformatics 30:1236–1240. https://doi.org/10.1093/bioinformatics/btu031.
87. Haft DH, Selengut JD, White O. 2003. The TIGRFAMs database of protein families. Nucleic Acids Res 31:371–373.
88. Overbeek R, Olson R, Pusch GD, Olsen GJ, Davis JJ, Disz T, Edwards RA, Gerdes S, Parrello B, Shukla M, Vonstein V, Wattam AR, Xia F, Stevens R. 2014. The SEED and the Rapid Annotation of microbial genomes using Subsystems Technology (RAST). Nucleic Acids Res 42:D206–D214. https://doi.org/10.1093/nar/gkt1226.
89. Galperin MY, Makarova KS, Wolf YI, Koonin EV. 2015. Expanded microbial genome coverage and improved protein family annotation in the COG database. Nucleic Acids Res 43:D261–D269. https://doi.org/10.1093/nar/gku1223.
90. Langmead B, Salzberg SL. 2012. Fast gapped-read alignment with Bowtie 2. Nat Methods 9:357–359. https://doi.org/10.1038/nmeth.1923.
91. Liao Y, Smyth GK, Shi W. 2014. featureCounts: an efficient general purpose program for assigning sequence reads to genomic features. Bioinformatics 30:923–930. https://doi.org/10.1093/bioinformatics/btt656.
92. Love MI, Huber W, Anders S. 2014. Moderated estimation of fold change

and dispersion for RNA-seq data with DESeq2. Genome Biol 15:550. https://doi.org/10.1186/s13059-014-0550-8.

93. R Core Team. 2017. R: a language and environment for statistical computing. R Foundation for Statistical Computing, Vienna, Austria.
94. Loy A, Küsel K, Lehner A, Drake HL, Wagner M. 2004. Microarray and functional gene analyses of sulfate-reducing prokaryotes in low-sulfate, acidic fens reveal cooccurrence of recognized genera and novel lineages. Appl Environ Microbiol 70:6998–7009. https://doi.org/10.1128/AEM.70.12.6998-7009.2004.
95. Katoh K, Standley DM. 2013. MAFFT multiple sequence alignment software version 7: improvements in performance and usability. Mol Biol Evol 30:772–780. https://doi.org/10.1093/molbev/mst010.
96. Huerta-Cepas J, Szklarczyk D, Forslund K, Cook H, Heller D, Walter MC, Rattei T, Mende DR, Sunagawa S, Kuhn M, Jensen LJ, von Mering C, Bork P. 2016. eggNOG 4.5: a hierarchical orthology framework with improved functional annotations for eukaryotic, prokaryotic and viral sequences. Nucleic Acids Res 44:D286–D293. https://doi.org/10.1093/nar/gkv1248.